Applied Catalysis B: Environmental 89 (2009) 577–582

Contents lists available at ScienceDirect

Applied Catalysis B: Environmental

journal homepage: www.elsevier.com/locate/apcatb

Self-assembly of $Bi_xTi_{1-x}O_2$ visible photocatalyst with core–shell structure and enhanced activity

Zhenfeng Bian [a], Jie Ren [a], Jian Zhu [a], Shaohua Wang [a], Yunfeng Lu [b,**], Hexing Li [a,*]

[a] Department of Chemistry, Shanghai Normal University, Shanghai 200234, PR China
[b] Chemical & Biomolecular Engineering Department, University of California, Los Angeles, CA 90095, USA

ARTICLE INFO

Article history:
Received 18 November 2008
Received in revised form 5 January 2009
Accepted 22 January 2009
Available online 2 February 2009

Keywords:
$Bi_xTi_{1-x}O_2$ visible photocatalyst
Core–shell structure
Solvothermal
Photodegradation of p-chlorophenol
Multiple reflections promoting effects

ABSTRACT

Mesoporous $Bi_xTi_{1-x}O_2$ spheres with core–shell chamber were prepared by alcoholysis under solvothermal conditions. The cross-condensation between Ti–OH and Bi–OH ensured complete incorporation of Bi-dopants into TiO_2 lattice, though Bi atom is much bigger than Ti. Meanwhile, the aggregation of titania building clusters into spheres and their subsequent reactions including dissolution and re-deposition processes lead to the hollow spheres with tunable interior structure. The Bi-doping induced strong spectral response in visible region owing to the formation of narrow intermediate energy band gaps. Meanwhile, multiple reflections within the sphere interior voids promoted the light absorbance. As a result, the as-prepared $Bi_xTi_{1-x}O_2$ spheres exhibited much higher activity than the undoped TiO_2, the Bi_2O_3/TiO_2 obtained by impregnating the TiO_2 with $Bi(NO_3)_3$ solution, and the $Bi_xTi_{1-x}O_2$ after being ground during photodegradation of p-chlorophenol under visible light irradiation. Meanwhile, the $Bi_xTi_{1-x}O_2$ could be used repetitively for 10 times owing to the high hydrothermal stability and the absence of Bi-leaching.

1. Introduction

Photocatalysis has caused much attention owing to its potential applications in environmental cleaning and H-energy production. TiO_2 is one of the most frequently used photocatalysts owing to its cheapness, non-toxicity, high stability, and easy preparation [1]. However, pure TiO_2 could be activated only by UV lights due to its big energy gap (3.0–3.2 eV) [2] and also exhibits low quantum efficiency in photocatalytic reactions due to the rapid recombination of photocharges [3]. To date, a great number of attempts have been made to achieve visible photocatalysts. Most studies are focused on doping TiO_2 with nonmetal and/or metal ions [4–10], noble metals [11,12], semiconductor oxides [13,14], and organic sensitizers [15]. It has been reported that the Bi_2O_3/TiO_2 displays strong visible lights owing to the narrow energy gap of Bi_2O_3 (2.8 eV) [6]. Since the Bi atom (103 pm) is much bigger than the Ti atom (61 pm) [16], the Bi_2O_3 is mainly present in a separated phase, which might limit the catalyst durability due to the leaching of Bi_2O_3 species. In comparison with the improvement of the spectral response in visible area, however, relatively little attention has been paid to enhance light absorbance by fabricating unique shape and morphology [17]. Herein, we develop a new approach to prepare Bi-doped TiO_2 photocatalyst by alcoholysis under solvothermal condition which ensures the complete incorporation of Bi-dopants into the TiO_2 lattice. Meanwhile, the interior structure could be tailored from solid, core–shell structured and hollow chambers with mesoporous outer surface. As a result, the as-prepared $Bi_xTi_{1-x}O_2$ exhibits high activity and strong durability during photocatalytic degradation of p-chlorophenol (4-CP) under visible irradiation.

2. Experimental

2.1. Catalyst preparation

All chemicals were analytical grade and used without further purification. In a typical run of catalyst synthesis, a clear solution containing $TiOSO_4$, glycerol, alcohol, $Bi(NO_3)_3{\cdot}5H_2O$ and ethyl ether (molar ratio = 1:16:40:*x*:11) was added into a 50-ml autoclave and kept at 110 °C for 48 h. The precipitate was filtered, washed thoroughly with absolute ethanol, dried at 100 °C, and calcined at a desired temperature for 4 h. The samples were denoted as *x*% $Bi_xTi_{1-x}O_2$, where *x* represents the Bi/Ti molar ratio. For comparison, other TiO_2 samples containing Bi^{3+} species (Bi/Ti molar ratio = 1.9%) were also prepared by impregnating the core–shell structured TiO_2 with $Bi(NO_3)_3$ solution and denoted as Bi_2O_3/TiO_2.

* Corresponding author. Tel.: +86 21 6432 2272; fax: +86 21 6432 2272.
** Corresponding author. Tel.: +1 310 794 7238; fax: +1 310 206 4107.
E-mail addresses: luucla@ucla.edu (Y. Lu), hexing-li@shnu.edu.cn (H. Li).

0926-3373/$ – see front matter © 2009 Elsevier B.V. All rights reserved.
doi:10.1016/j.apcatb.2009.01.014

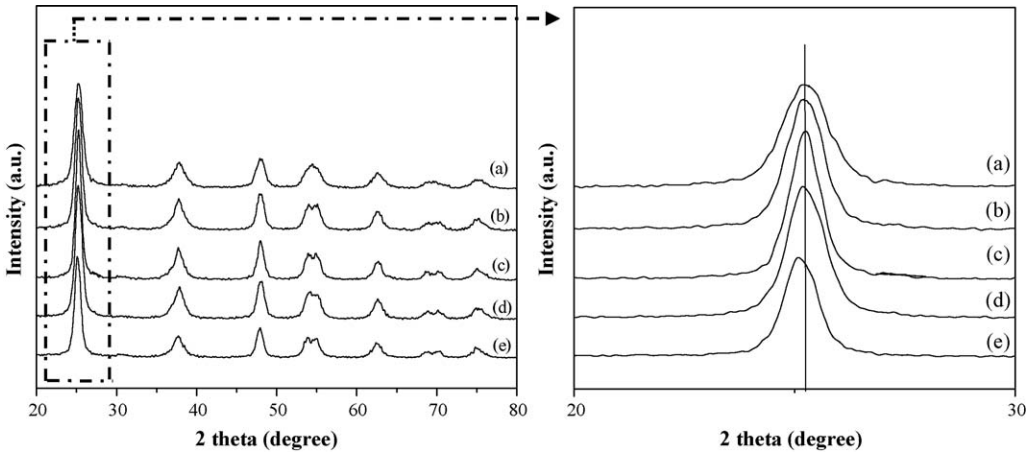

Fig. 1. XRD patterns of $Bi_xTi_{1-x}O_2$ samples with Bi/Ti molar ratio of (a) 0%, (b) 0.67%, (c) 1.1%, (d) 1.9%, and (e) 3.6%. All these samples have been calcined at 773 K for 4 h.

2.2. Catalyst characterization

The sample structure was determined by X-ray diffraction (XRD, D/MAX-2000 with Cu $K\alpha_1$ irradiation), scanning electron microscopy (SEM, JEOL JSM-6380LV) and transmission electronic micrograph (TEM, JEM-2010, operated at 200 kV), N_2 adsorption–desorption (Quantachrome NOVA 4000e, at 77 K). Based on the adsorption branches of N_2 sorption isotherms, the Brunauer–Emmett–Teller (BET) method was used to calculate the specific surface area (S_{BET}) and the Barrett–Joyner–Halenda (BJH) model was used to calculate pore volume (V_P), the average pore diameter (D_P), and the pore size distribution. Raman spectra were recorded using a Super LabRam-II spectrometer with a holographic grating of 1800 g/mm. Fourier transform infrared (FTIR) spectra were collected with a Nicolet Magna 550 spectrometer by using the KBr method. Thermal stability was evaluated by thermogravimetric analysis (TGA, DTG-60H) with a heating speed of 10 °C/min in air flow (50 ml/min). The ^{13}C NMR spectra were recorded on a Bruker AV-400. The surface electronic states were analyzed by X-ray photoelectron spectroscopy (XPS, Perkin-Elmer PHI 5000) and the Bi/Ti molar ratio was determined based on the area ratio of the principal XPS peaks in $Bi_{4f7/2}$ and $Ti_{2p3/2}$ levels using 5.65 and 1.0 as the PHI sensitivity factors, respectively [9]. All the binding energies were calibrated by using the contaminant carbon (C_{1s} = 284.6 eV) as a reference. The Bi-species leached during repetitive photocatalytic reactions were determined by inductively coupled plasma optical emission spectrometer (ICP, Varian VISTA-MPX).

2.3. Activity test

Photocatalytic degradation of p-chlorophenol was carried out at 30 °C in a 80-ml self-designed quartz reactor containing 0.080 g catalyst and 50 ml 4-CP aqueous solution (1.0×10^{-4} M). The mixture was stirred for 1 h until reaching adsorption equilibrium. Then, the photocatalysis was initiated by irradiating the system with a 500 W xenon lamp located at 18 cm away from the reaction solution. All the UV lights with wavelength shorter than 420 nm were removed by a glass filter (JB-420). After reaction for 6 h, the unreacted 4-CP was determined by the UV–vis spectroscopy (UV-7504PC) at its characteristic wavelength of 224 nm [18], from which the degradation yield could be calculated. The TOC analysis confirmed the complete degradation of 4-CP to carbon dioxides. Preliminary tests demonstrated a good linear relationship between the light absorbance and the 4-CP concentration. Only less than 3% 4-CP decomposed after reaction for 6 h in the absence of either the photocatalyst or the visible light, which could be neglected in comparison with the photodegradation yield. The reproducibility of the results was checked by repeating the results at least three times and was found to be within acceptable limits (±5%).

3. Results and discussion

The XRD patterns (Fig. 1) revealed that all the undoped TiO_2 and $Bi_xTi_{1-x}O_2$ samples displayed well-crystallized anatase phase after being calcined at 773 K for 4 h. The $Bi_xTi_{1-x}O_2$ underwent phase transformation from anatase to rutitle at calcination temperature of 973 K, nearly 50 K higher than the undoped TiO_2 (Fig. S1), showing an excellent thermal stability. The Bi-doping resulted in a negative shift of the principal peak, indicating the crystal distortion which could be attributed to the incorporation of Bi-species into the TiO_2 lattice. However, impregnation of the TiO_2 with $Bi(NO_3)_3$ solution causes no significant shift of the principal XRD peak (Fig. S2), implying that the Bi-species are present in a separated phase of Bi_2O_3. FTIR spectra (Fig. S3) further confirmed the formation of –Ti–O–Bi– bonds in the $Bi_xTi_{1-x}O_2$ sample, corresponding to the absorbance band around 1459 cm^{-1}. It is well-known that the Bi atom (103 pm) is much bigger than the Ti atom (61 pm) [16]. Thus, the Bi-species could not incorporate into the TiO_2 lattice during regular sol–gel route [6,19]. However, owing to the high pressure and temperature under solvothermal conditions,

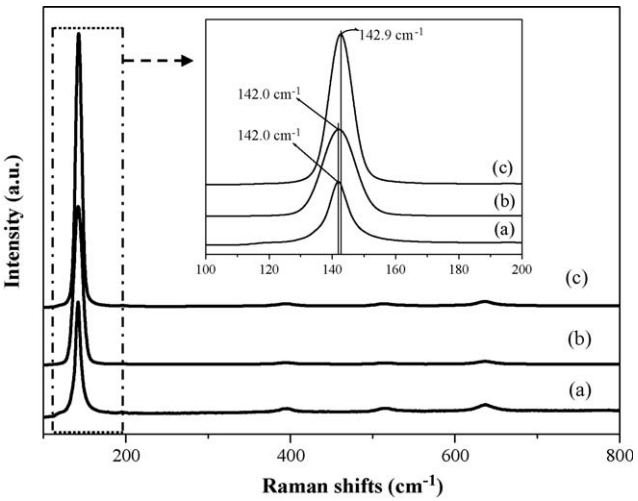

Fig. 2. Raman spectra of (a) TiO_2, (b) 1.9% Bi_2O_3/TiO_2, and (c) 1.9% $Bi_xTi_{1-x}O_2$ samples calcined at 773 K.

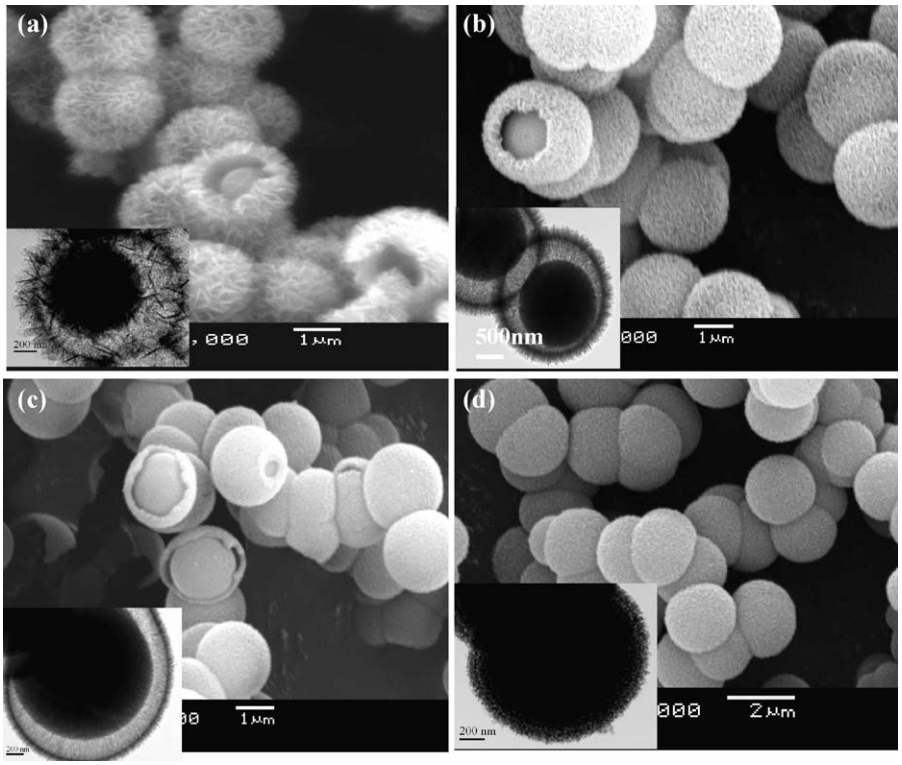

Fig. 3. SEM and TEM (inset) images of $Bi_xTi_{1-x}O_2$ samples with Bi/Ti molar ratio of (a) 0%, (b) 0.67%, (c) 1.9%, and (d) 3.6%. All these samples have been calcined at 773 K for 4 h.

the cross-condensation between Bi–OH and Ti–OH occurred to form –Ti–O–Bi– bonds (see Scheme S1), which ensured the complete incorporation of Bi-species into the TiO_2 lattice. Further evidences could be supplied from Raman spectra. As shown in Fig. 2, all the TiO_2, Bi_2O_3/TiO_2 and $Bi_xTi_{1-x}O_2$ samples displayed an intensive peak indicative of the anatase phase [20]. However, the $Bi_xTi_{1-x}O_2$ showed a positive shift by 0.9 cm^{-1}, implying the increase in the number of surface oxygen vacancies [20]. This again confirmed the incorporation of Bi-species into the TiO_2 lattice via forming –Ti–O–Bi– bonds, leading to the decrease of O/Ti ratio in the $Bi_xTi_{1-x}O_2$ sample since the Bi-species were present in +3 valence while the Ti-species were in +4 valence.

The SEM and TEM images (Fig. 3) demonstrated that all the undoped TiO_2 and $Bi_xTi_{1-x}O_2$ samples with Bi/Ti molar ratio $<3.6\%$ display core–shell structured spheres. Impregnation of the TiO_2 with $Bi(NO_3)_3$ solution had no significant influence on the core–shell structure (see Fig. S4). The HRTEM image (Fig. S5) demonstrated that the $Bi_xTi_{1-x}O_2$ calcined at 773 K displayed well-crystallized anatase phase with the lattice distance around 0.36 nm [21]. While, the mapping image clearly displayed the uniform distribution of the Bi-species in the $Bi_xTi_{1-x}O_2$ sample (see Fig. S6). Increase of Bi-content results in a slight shrinkage of the outer shell while the inside core remains almost unchanged. At Bi/Ti $> 3.6\%$, only solid spheres are observed since the diameter of the outer shell decreased to the same size of the interior core. From Fig. 4 one could see that all the TiO_2, $Bi_xTi_{1-x}O_2$ and Bi_2O_3/TiO_2 samples displayed type-IV N_2 adsorption–desorption isotherms with H_1 hysteresis indicative of the mesoporous structure [22]. The inset showed that the 1.9% $Bi_xTi_{1-x}O_2$ exhibited a narrow pore size distribution centered at 11 nm.

The formation of core–shell structure in the TiO_2 and the $Bi_xTi_{1-x}O_2$ samples could be mainly attributed to the alcoholysis-induced self-assembly under solvothermal conditions, involving the aggregation of titania building clusters into spheres and their subsequent reaction, dissolution and re-deposition processes [17,23]. As shown in Fig. 5a, solid spheres formed at initial stage through alcoholysis and condensation reactions of $TiOSO_4$. During the solvothermal condition, etherifying reactions among alcohol and glycerol produced water continuously. This has been confirmed by GC–MS and NMR which evidenced the formation of ethyl ether and the ethers from ethanol and glycerol (Figs. S7 and S8). Since the solid TiO_2 spheres contained a large number of hydrolysable organic species (e.g., R–SO_4, glyceroxy and ethoxy groups) due to slow reaction kinetics, the as-formed water might induce the further hydrolysis of organics capsulated in the TiO_2 spheres, leading to the dissolution and rearrangement of the titania building clusters. Resulted from this process, surface plates were initially formed and grown into an outside sphere and an inside core (Fig. 5b). Continuation of such processes gradually dissolved the core spheres, leading to the hollow spheres (Fig. 5c).

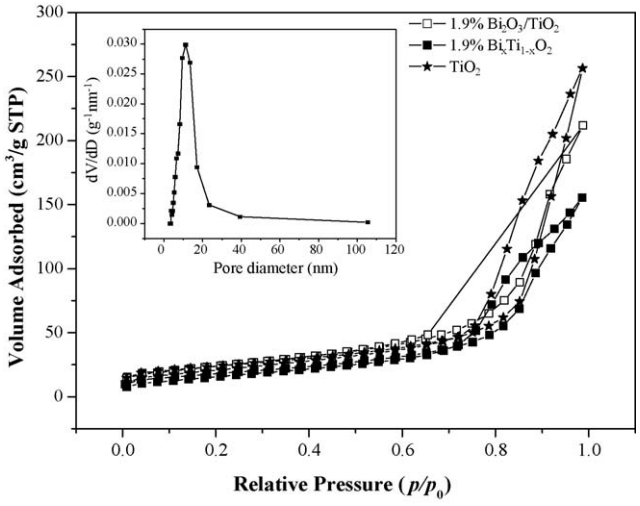

Fig. 4. N_2 adsorption–desorption isotherms of different samples calcined at 773 K. The inset is pore diameter distribution of the 1.9% $Bi_xTi_{1-x}O_2$.

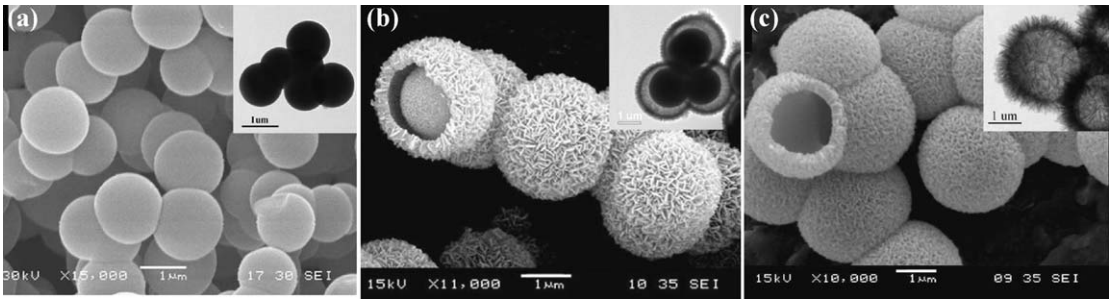

Fig. 5. SEM and TEM (inset) images of the TiO_2 samples obtained after alcoholysis under solvothermal conditions for (a) 1 h, (b) 48 h, and (c) 336 h, respectively.

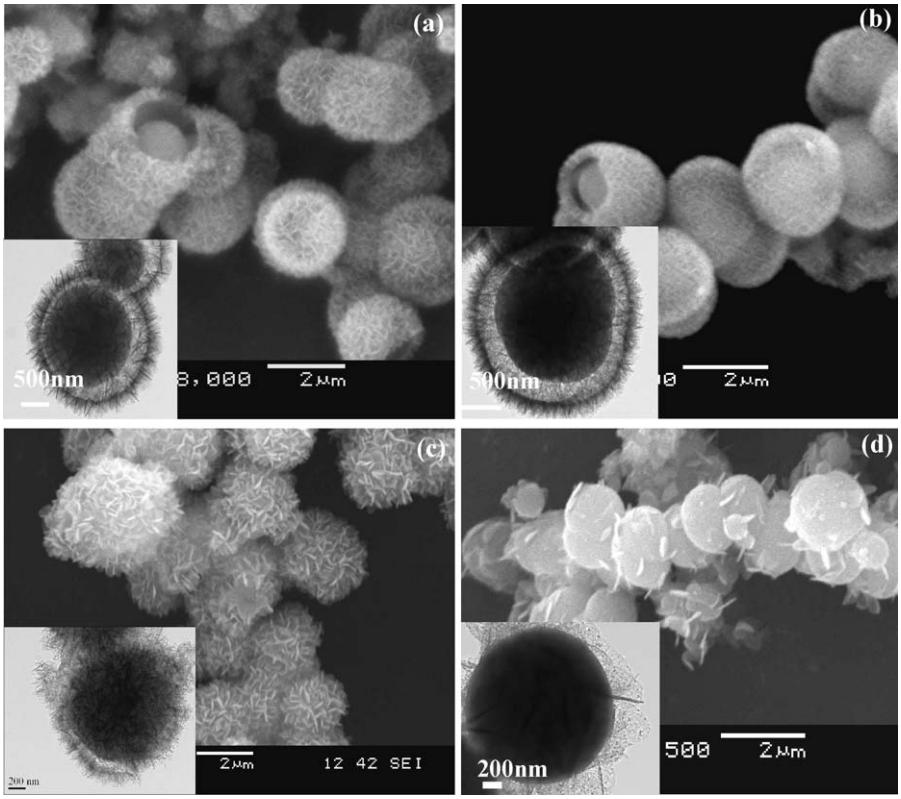

Fig. 6. SEM and TEM (inset) images of the TiO_2 spheres obtained by alcoholysis under solvothermal conditions for 48 h in the presence of (a) 7.7 μl H_2O, (b) 100 μl H_2O, (c) 0.5 ml H_2O, and (d) 1.0 ml H_2O. All samples were calcined at 773 K for 4 h.

The stepwise hydrolysis and dissolution of organic species could be confirmed by TG/DTA (Fig. S9) which revealed that the initial TiO_2 spheres show multiple exothermic peaks with the weight loss of 60%, while the TiO_2 spheres obtained after being treated under solvothermal conditions for 48 h exhibited only one small exothermic peak with the weight loss less than 10%. The FTIR spectra (Fig. S10) revealed that, the initial TiO_2 sample displayed stronger absorbance peaks around 1000–1500 cm^{-1} indicative of C–C and/or C–O bonds [24], implying the presence of large amount of organic species. After being treated for 48 h under solvothermal conditions, these peaks diminished due to stepwise hydrolysis and dissolution of organic species. The mesoporous structure was commonly observed in the TiO_2 samples obtained by alcoholysis, which could be attributed to the structure-directing effect from glycol [25,26]. The $Bi_xTi_{1-x}O_2$ displayed transformation from core–shell structure to solid structure with the increase of Bi-content up to 3.6%. This could be attributed to the increase of crystal water in $Bi(NO_3)_3{\cdot}5H_2O$ which disturbed the stepwise hydrolysis. A direct evidence could be obtained by adding elevated amount of water during alcoholysis of $TiOSO_4$ under solvothermal conditions. As shown in Fig. 6, both the SEM and TEM images clearly showed the

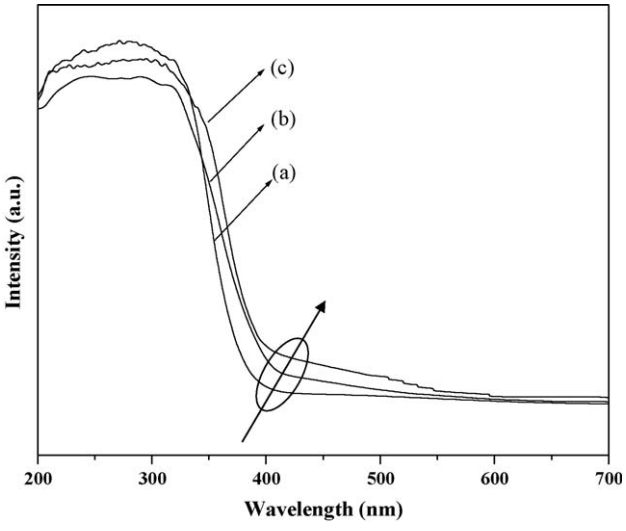

Fig. 7. UV–vis DRS spectra of (a) TiO_2, (b) 1.9% Bi_2O_3/TiO_2, and (c) 1.9% $Bi_xTi_{1-x}O_2$ samples calcined at 773 K.

Table 1
Structural parameters and activities of different photocatalysts[a].

Sample	Calcination temperature (K)	S_{BET} (m^2/g)	D_P (nm)	V_P (cm^3/g)	Degradation (%)
TiO_2	773	86	13	0.43	11
0.67% $Bi_xTi_{1-x}O_2$	773	84	11	0.40	33
1.1% $Bi_xTi_{1-x}O_2$	773	81	10	0.36	46
1.9% $Bi_xTi_{1-x}O_2$	773	79	11	0.31	55
3.6% $Bi_xTi_{1-x}O_2$	773	64	9.2	0.21	21
1.9% $Bi_xTi_{1-x}O_2$	723	97	7.2	0.33	35
1.9% $Bi_xTi_{1-x}O_2$	873	56	14	0.27	43
1.9% $Bi_xTi_{1-x}O_2$	973	36	17	0.10	11
1.9% Bi_2O_3/TiO_2	773	56	8.9	0.18	33
1.9% $Bi_xTi_{1-x}O_2$ (ground)	773	88	10	0.35	43

[a] Reaction conditions: 0.080 g photocatalyst, 50 ml aqueous solution containing 10 mg/l 4-CP, a 500 W Xe lamp at 18 cm away from the reaction solution (the wavelength less than 420 nm were removed by a glass filter), reaction temperature = 298 K, stirring rate = 1000 rpm, reaction period = 6 h.

transformation from core–shell structured spheres to solid spheres with the increase of water.

The UV–vis DRS spectra (Fig. 7) demonstrated that the pure TiO_2 displayed no absorbance in visible area, which could be easily understood by considering its big energy gap between the conduction band and the valence band (3.2 eV). The Bi_2O_3/TiO_2 showed absorbance for visible lights owing to the photosensitizing effect of Bi_2O_3 [6,27]. The $Bi_xTi_{1-x}O_2$ exhibited spectral response in visible area owing to the formation of intermediate energy levels between the top of the (lone pair) Bi^{3+} 6s band and the bottom of the Ti^{4+} 3d band [28], leading to the narrow energy gaps. The $Bi_xTi_{1-x}O_2$ exhibited stronger absorbance for visible lights than the Bi_2O_3/TiO_2 owing to the stronger Bi-doping effect than the Bi_2O_3 photosensitizing effect.

Other structural parameters were listed in Table 1. The S_{BET}, V_P and D_P values of the $Bi_xTi_{1-x}O_2$ decreased gradually with the increase of Bi-content, which could be attributed to the sphere shrinkage. At Bi/Ti molar ratio of 3.6%, the $Bi_xTi_{1-x}O_2$ sample turned to be solid spheres, leading to abrupt decrease in S_{BET}, V_P and D_P. The Bi_2O_3/TiO_2 exhibited lower S_{BET}, V_P and D_P than the $Bi_xTi_{1-x}O_2$ since the Bi_2O_3 species covered the surface and partially block the mesoporous channels. Calcination of the $Bi_xTi_{1-x}O_2$ at elevated temperatures caused decreases in both the S_{BET} and the V_P due to the sphere shrinkage.

Table 1 summarized activities of different samples during liquid phase photocatalytic degradation of 4-CP under visible light irradiation. With the increase of calcination temperature, the activity of the $Bi_xTi_{1-x}O_2$ first increased and then decreased. The maximum activity was obtained at 773 K. Taking into account that the S_{BET} decreased monotonously with the enhanced calcination temperature, the increase in photocatalytic activity of the 1.9% $Bi_xTi_{1-x}O_2$ calcined up to 773 K could be mainly attributed to the enhanced crystallization degree of anatase which may facilitate electron transfer from bulk to surface and thus inhibit their recombination with photo-induced holes, leading to the higher quantum efficiency [7–10]. Further increase of the calcination temperature caused decrease in photocatalytic activity due to significant decrease of S_{BET} and the collapse of the mesoporous channels. Abrupt decrease in activity was observed at 973 K, obviously due to the transformation from anatase to rutile. The $Bi_xTi_{1-x}O_2$ exhibited much higher activity than the pure TiO_2 owing to the spectral response in visible area. The activity increased with the enhanced Bi-content owing to the formation of more intermediate energy levels, making $Bi_xTi_{1-x}O_2$ easier to be activated by visible lights. The maximum activity was obtained at Bi/Ti molar ratio of 1.9%. Further increase of the Bi/Ti molar ratio to 3.6% resulted in an abrupt decrease in the activity. Besides the decrease in S_{BET}, the disappearance of core–shell structure was mainly responsible for the decrease of photocatalytic activity since such core–shell structure could make better use of lights via a multi-reflection model (see Scheme 1). This was strongly supported by the evidence that the ground $Bi_xTi_{1-x}O_2$ exhibited much lower activity, though its S_{BET} slightly increased. With the same Bi-content (Bi/Ti molar ratio = 1.9%), the $Bi_xTi_{1-x}O_2$ exhibited much higher activity than the Bi_2O_3/TiO_2 obtained via impregnation, which could be attributed to the higher surface area and the stronger spectral response in visible area owing to the incorporation of Bi-species into the TiO_2 lattice.

The recycling test (Fig. 8) revealed that the $Bi_xTi_{1-x}O_2$ exhibited no significant decrease in activity after being used repetitively for 10 times, indicating the high hydrothermal stability of the mesoporous/

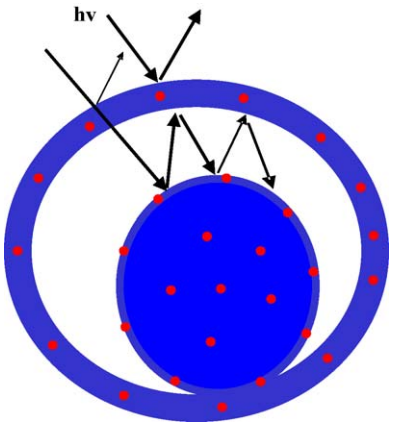

Scheme 1. Schematic illustration of the light multi-reflections in the core–shell structured chamber of the $Bi_xTi_{1-x}O_2$. Red dots = Bi^{3+}, blue area = TiO_2. (For interpretation of the references to colour in this legend, the reader is referred to the web version of the article.)

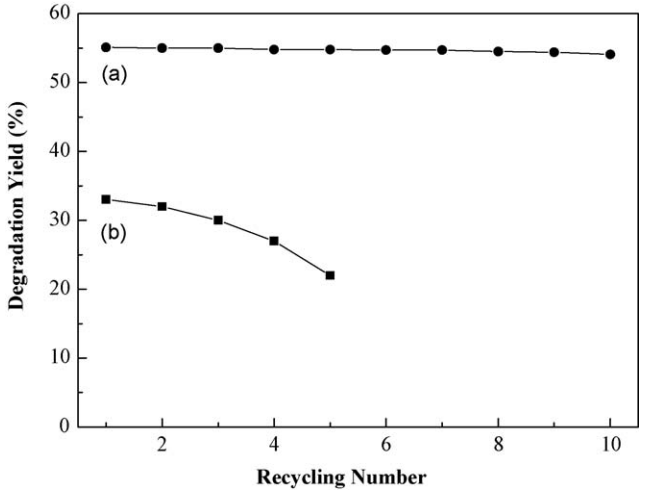

Fig. 8. Recycling test of (a) 1.9% $Bi_xTi_{1-x}O_2$ and (b) 1.9% Bi_2O_3/TiO_2 catalysts calcined at 773 K. Reaction conditions are given in Table 1.

core–shell structure and the lack of Bi-leaching owing to the strong incorporation into the TiO_2 lattice. The ICP analysis demonstrated that only 0.040% Bi-species were leached after the $Bi_xTi_{1-x}O_2$ was used repetitively for 10 times. However, the activity of the Bi_2O_3/TiO_2 decreased rapidly within five recycles due to the leach of Bi-species. The ICP analysis demonstrated that the Bi-content in the Bi_2O_3/TiO_2 decreased by 11% after being used repetitively for 10 times.

4. Conclusions

The present work developed a new approach to synthesize mesoporous $Bi_xTi_{1-x}O_2$ spheres with core–shell structure based on alcoholysis under solvothermal conditions. The incorporation of the Bi-species into the TiO_2 lattice generated new intermediate energy levels, leading to the spectral response in visible area. While the core–shell structure promoted the utilization of lights via multi-reflections. As a result, the $Bi_xTi_{1-x}O_2$ exhibited high activity during liquid phase photocatalytic degradation of p-chlorophenol under irradiation of visible lights. Besides, the $Bi_xTi_{1-x}O_2$ also showed strong durability and could be used repetitively for more than 10 times. The alcoholysis under solvothermal conditions allowed the *in situ* doping and self-assembling hierarchical structures, which offers more opportunities to design new functional materials.

Acknowledgments

This work was supported by the National Natural Science Foundation of China (20825724) and Shanghai Government (S30406, 07dz22303, and 0852nm01000).

Appendix A. Supplementary data

Supplementary data associated with this article can be found, in the online version, at doi:10.1016/j.apcatb.2009.01.014.

References

[1] A. Fujishima, T.N. Rao, D.A. Tryk, J. Photochem. Photobiol. C 1 (2000) 1–21.
[2] J.C. Yu, G.S. Li, X.C. Wang, X.L. Hu, C.W. Leung, Z.D. Zhang, Chem. Commun. (2006) 2717–2719.
[3] I. Justicia, P. Ordejón, G. Canto, J.L. Mozos, J. Fraxedas, G.A. Battiston, R. Gerbasi, A. Figueras, Adv. Mater. 14 (2002) 1399–1402.
[4] R. Asahi, T. Morikawa, T. Ohwaki, K. Aoki, Y. Taga, Science 293 (2001) 269–271.
[5] W. Choi, A. Termin, M.R. Hoffmann, J. Phys. Chem. 98 (1994) 13669–13679.
[6] Z.F. Bian, J. Zhu, S.H. Wang, Y. Cao, X.F. Qian, H.X. Li, J. Phys. Chem. C 112 (2008) 6258–6262.
[7] H.X. Li, X.Y. Zhang, Y.N. Huo, J. Zhu, Environ. Sci. Technol. 41 (2007) 4410–4414.
[8] H.X. Li, J.X. Li, Y.N. Huo, J. Phys. Chem. B 110 (2006) 1559–1565.
[9] Y.N. Huo, Z.F. Bian, X.Y. Zhang, Y. Jin, J. Zhu, H.X. Li, J. Phys. Chem. C 112 (2008) 6546–6550.
[10] Y.N. Huo, X.Y. Zhang, Y. Jin, J. Zhu, H.X. Li, Appl. Catal. B: Environ. 83 (2008) 78–84.
[11] H.X. Li, Z.F. Bian, J. Zhu, Y.N. Huo, H. Li, Y.F. Lu, J. Am. Chem. Soc. 129 (2007) 4538–4539.
[12] J. Kim, D. Lee, J. Am. Chem. Soc. 129 (2007) 7706–7707.
[13] I. Robel, V. Subramanian, M. Kuno, P.V. Kamat, J. Am. Chem. Soc. 128 (2006) 2385–2393.
[14] R. Vogel, P. Hoyer, H. Weller, J. Phys. Chem. 98 (1994) 3183–3188.
[15] O.B. Regan, M. Gratzel, Nature 353 (1991) 737–740.
[16] S. Rengaraj, X.Z. Li, P.A. Tanner, Z.F. Pan, G.K. Pang, J. Mol. Catal. A 247 (2006) 36–43.
[17] H.X. Li, Z.F. Bian, J. Zhu, D.Q. Zhang, G.S. Li, Y.N. Huo, H. Li, Y.F. Lu, J. Am. Chem. Soc. 129 (2007) 8406–8407.
[18] S. Sakthivel, H. Kisch, Angew. Chem. Int. Ed. 42 (2003) 4908–4911.
[19] J. Zhang, M.J. Li, Z.C. Feng, J. Chen, C. Li, J. Phys. Chem. B 110 (2006) 927–935.
[20] J.C. Parker, R.W. Siegei, Appl. Phys. Lett. 57 (1990) 943–945.
[21] K. Nagaveni, M.S. Hegde, N. Ravishankar, G.N. Subbanna, G. Madras, Langmuir 20 (2004) 2900–2907.
[22] T. Yu, H. Zhang, X.W. Yan, Z.X. Chen, X.D. Zou, P. Oleynikov, D.Y. Zhao, J. Phys. Chem. B 110 (2006) 21467–21472.
[23] H.C. Zeng, J. Mater. Chem. 16 (2006) 649–662.
[24] S.J. Bu, Z.G. Jin, X.X. Liu, H.Y. Du, Z.J. Cheng, J. Sol-Gel Sci. Technol. 30 (2004) 239–248.
[25] J. Zhu, J. Ren, Y.N. Huo, Z.F. Bian, H.X. Li, J. Phys. Chem. C 111 (2007) 18965–18969.
[26] J. Zhu, J. Yang, Z.F. Bian, Y. Liu, J. Ren, Y. Cao, H.X. Li, Appl. Catal. B: Environ. 76 (2007) 82–91.
[27] Y. Bessekhouad, D. Robert, J.V. Weber, Catal. Today 101 (2005) 315–321.
[28] W.F. Yao, H. Wang, X.H. Xu, X.F. Cheng, J. Huang, S.X. Shang, X.N. Yang, M. Wang, Appl. Catal. A: Gen. 243 (2003) 185–190.